mortality trends. Data from the Office of National Statistics suggest that the number of deaths assigned to the respiratory chapter as a whole decreased by 22% as a result of the introduction of ICD-10 codes, largely driven by the decrease in number of deaths assigned to pneumonia (10). It is possible that this may have resulted in further underestimating the actual number of IPF-CS–related deaths.

These findings are consistent with our work demonstrating a progressive increase in IPF mortality in the United Kingdom (1, 2, 11). Increased case ascertainment could be a contributing factor to the trends seen, but it is also possible that the true incidence of IPF has continued to increase. If the marked increase in number of deaths is purely due to increased disease recognition, there is no evidence that ascertainment is complete, and continued upward trends in mortality are likely to be seen.

In summary, IPF-CS now accounts for almost 7% of all respiratory deaths in the United Kingdom (4) and carries the same mortality burden as liver, bladder, and intracranial malignancies. Despite increasing research investment, it remains an important cause of respiratory mortality and a growing public health problem. ■

Author disclosures are available with the text of this letter at www.atsjournals.org.

Acknowledgment: The authors thank Joe West for extracting and providing the data used in the study.

Vidya Navaratnam, B.M. B.S., Ph.D.*
University of Nottingham
Nottingham, United Kingdom
and
Menzies School of Health Research
Darwin, Australia

Richard B. Hubbard, M.B. B.S., M.D.
University of Nottingham
Nottingham, United Kingdom

ORCID ID: 0000-0002-2914-8012 (V.N.).

*Corresponding author (e-mail: vidya.navaratnam@nottingham.ac.uk).

References

1. Navaratnam V, Fleming KM, West J, Smith CJ, Jenkins RG, Fogarty A, *et al*. The rising incidence of idiopathic pulmonary fibrosis in the U.K. *Thorax* 2011;66:462–467.
2. Hutchinson JP, McKeever TM, Fogarty AW, Navaratnam V, Hubbard RB. Increasing global mortality from idiopathic pulmonary fibrosis in the twenty-first century. *Ann Am Thorac Soc* 2014;11:1176–1185.
3. Johnston I, Britton J, Kinnear W, Logan R. Rising mortality from cryptogenic fibrosing alveolitis. *BMJ* 1990;301:1017–1021.
4. Office for National Statistics. Datasets related to deaths [accessed 2019 Feb 7]. Available from: https://www.ons.gov.uk/peoplepopulation andcommunity/birthsdeathsandmarriages/deaths#datasets.
5. Office for National Statistics. Mortality statistics in England and Wales QMI [updated 2018 Jul; accessed 2019 Feb 5]. Available from: https://www.ons.gov.uk/peoplepopulationandcommunity/birthsdeathsandmarriages/deaths/methodologies/mortalitystatisticsinenglandandwalesqmi.
6. Office for National Statistics. Death certification reform: a case study on the potential impact on mortality statistics, England and Wales. Statistical Bulletin; 2012.
7. Navaratnam V, Fogarty AW, Glendening R, McKeever T, Hubbard RB. The increasing secondary care burden of idiopathic pulmonary fibrosis: hospital admission trends in England from 1998 to 2010. *Chest* 2013;143:1078–1084.
8. Raghu G, Remy-Jardin M, Myers JL, Richeldi L, Ryerson CJ, Lederer DJ, *et al*.; American Thoracic Society; European Respiratory Society; Japanese Respiratory Society; Latin American Thoracic Society. Diagnosis of idiopathic pulmonary fibrosis: an official ATS/ERS/JRS/ALAT clinical practice guideline. *Am J Respir Crit Care Med* 2018;198: e44–e68.
9. Coultas DB, Hughes MP. Accuracy of mortality data for interstitial lung diseases in New Mexico, USA. *Thorax* 1996;51:717–720.
10. Brock A, Griffiths C, Rooney C. The impact of introducing ICD-10 on analysis of respiratory mortality trends in England and Wales. *Health Stat Q* 2006;(29):9–17.
11. Hubbard R, Johnston I, Coultas DB, Britton J. Mortality rates from cryptogenic fibrosing alveolitis in seven countries. *Thorax* 1996;51: 711–716.

Type I Collagen–targeted Positron Emission Tomography Imaging in Idiopathic Pulmonary Fibrosis: First-in-Human Studies

To the Editor:

Excessive collagen deposition is a hallmark of idiopathic pulmonary fibrosis (IPF). Although conventional imaging modalities, such as computed tomography (CT), can visualize the end results of collagen deposition, including reticular opacities and honeycombing, direct collagen visualization currently requires histopathology. We developed a positron emission tomography (PET) radiotracer, termed ^{68}Ga-CBP8, that binds specifically to type I collagen (1). In a mouse model of bleomycin-induced lung injury, we showed that ^{68}Ga-CBP8 can detect and quantify the degree of pulmonary fibrosis, and in a second mouse model, we showed that ^{68}Ga-CBP8 PET can measure treatment response with an anti-$\alpha v\beta 6$ antibody. Additionally, ^{68}Ga-CBP8 signal was highly correlated with the amount of collagen in explanted human IPF lungs as determined by the percentage of Sirius Red staining. Here, we present the results of the first-in-human studies using ^{68}Ga-CBP8 to assess safety and tracer distribution in healthy volunteers, and the ability to noninvasively measure increased lung collagen in subjects with IPF. Some of the results of these studies have been previously reported in the form of an abstract (2).

Methods

This study was approved by the Partners Institutional Review Board and registered at clinicaltrials.gov (identifier: NCT03535545). All of the subjects provided informed consent. Healthy volunteers were

Supported by NIH grant R01HL131907 (P.C. and M.L.). S.B.M. is supported by grants from the Francis Family Foundation and the Scleroderma Foundation.

Author Contributions: S.B.M., P.D., M.L., P.C., and C.C. designed the study. S.B.M., D.I.-G., E.A., L.L.L., S.D., R.S., P.C., and C.C. performed data collection, analysis, and/or interpretation. S.B.M. and C.C. performed statistical analyses, had full access to all of the data, and were responsible for the decision to submit for publication. S.B.M. drafted the manuscript. All authors contributed to a critical review of the manuscript and provided final approval for submission.

Originally Published in Press as DOI: 10.1164/rccm.201903-0503LE on June 4, 2019

without pulmonary disease, and all but one were nonsmokers (after completion of the study, one subject was found to have a history of tobacco use). Subjects with IPF had not used tobacco within the past 6 months. All subjects were excluded for contraindications to undergoing magnetic resonance imaging, respiratory infection within the prior 6 weeks, and prior radiation therapy to the thorax.

^{68}Ga-CBP8 PET and magnetic resonance imaging were performed simultaneously using the Siemens Biograph mMR scanner (Siemens Healthineers). Healthy volunteers underwent whole-body scanning, and subjects with IPF underwent scanning of the thorax. The subjects were monitored continuously during the imaging study and contacted the following day to assess for any adverse effects. Approximately 250 MBq (range 156–433 MBq) of ^{68}Ga-CBP8 was administered. Emission data were acquired for up to 2 hours in listmode format. Attenuation correction was performed using the manufacturer's MR-based method. Images corresponding to dynamic frames were reconstructed using the standard reconstruction algorithm (OSEM, 21 subsets, three iterations, 256 × 256 matrix size, 127 slices) and smoothed with a 4-mm full width at half maximum Gaussian filter. Standardized uptake values (SUVs) were obtained from regions of interest defined by segmenting each lung into three equal parts in the axial direction and dividing each part into subpleural (the outer 1.8 cm of the lung) and central regions. We averaged SUVs from the left and right lungs at each measurement. Statistical analysis was performed using the Mann-Whitney *U* test (Prism 6.0, GraphPad Software), with P value < 0.05 considered significant. Data are reported as mean ± SD or median (range) as appropriate. PET images were constructed for visualization of collagen tracer signal intensity and compared with CT of the chest performed for clinical indications in the subjects with IPF.

Results

We imaged five healthy volunteers (three males and two females, age 62.2 ± 7.8 yr) and nine subjects with IPF (six males and three females, age 72.7 ± 6.1 yr). Eight of the nine subjects with IPF were on antifibrotic therapy (pirfenidone or nintedanib). All of the subjects tolerated ^{68}Ga-CBP8 without difficulty and with no unexpected adverse effects. One healthy volunteer (intravenous extravasation) and one subject with IPF (MR-based attenuation correction map failed) were excluded from SUV analyses. ^{68}Ga-CBP8 displayed rapid renal clearance with low background uptake in the lungs of healthy volunteers. Whole-lung SUVs were increased in subjects with IPF compared with healthy volunteers when measured 1 hour after injection (0.65 [0.51–0.72] vs. 0.48 [0.33–0.56], $P = 0.048$). Assessment for regional differences showed that SUVs for subjects with IPF were significantly increased in the middle subpleural and lower lung regions (Figure 1). In contrast to healthy volunteers, there was a trend toward the collagen tracer signal being more heterogeneous in subjects with IPF (coefficient of variation 15.4% [12.6–20.4] vs. 11.2% [9.3–17.3], $P = 0.1$). High collagen tracer signal was seen in fibrotic lung regions determined by chest CT and also in regions where the lung appeared to be normal on CT (Figure 2).

Discussion

We successfully performed the first noninvasive direct visualization of type I collagen in humans using ^{68}Ga-CBP8 PET. ^{68}Ga-CBP8 is safe and well tolerated, with favorable tracer characteristics. ^{68}Ga-CBP8 signal was increased in the lungs of subjects with IPF compared with healthy volunteers. The increased collagen tracer signal in IPF displayed a lower lung and subpleural predominance consistent with the anatomic distribution of IPF. Our findings add to a growing literature on the use of molecular imaging for noninvasive characterization and anatomic localization of fibrosis-related processes (3–6) and the use of PET for pulmonary fibrosis imaging (7–10).

Type I collagen is a key structural protein of the extracellular matrix. Excessive extracellular matrix accumulation is a pathogenic feature of fibrosis (11). ^{68}Ga-CBP8 binds type I human collagen with a K_d of 2.1 μM (1). Preclinical data suggest that ^{68}Ga-CBP8 may be more sensitive to recently synthesized collagen than to established collagen. Although the ^{68}Ga-CBP8 signal linearly correlated with lung collagen in pulmonary fibrosis models, it was much lower in

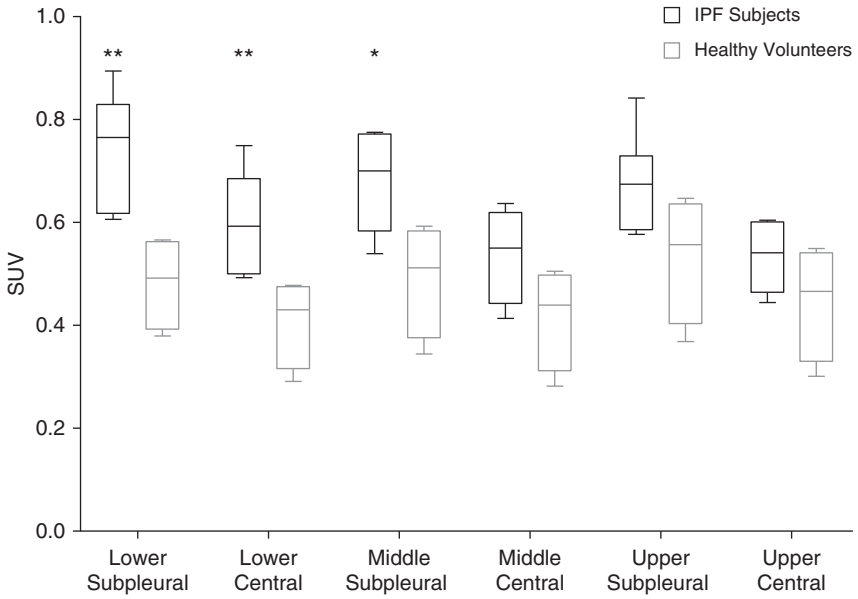

Figure 1. ^{68}Ga-CBP8 standardized uptake values (SUVs). Data are reported as box-and-whisker plots. *$P < 0.05$ and **$P < 0.01$ for subjects with idiopathic pulmonary fibrosis (IPF) compared with healthy volunteers.

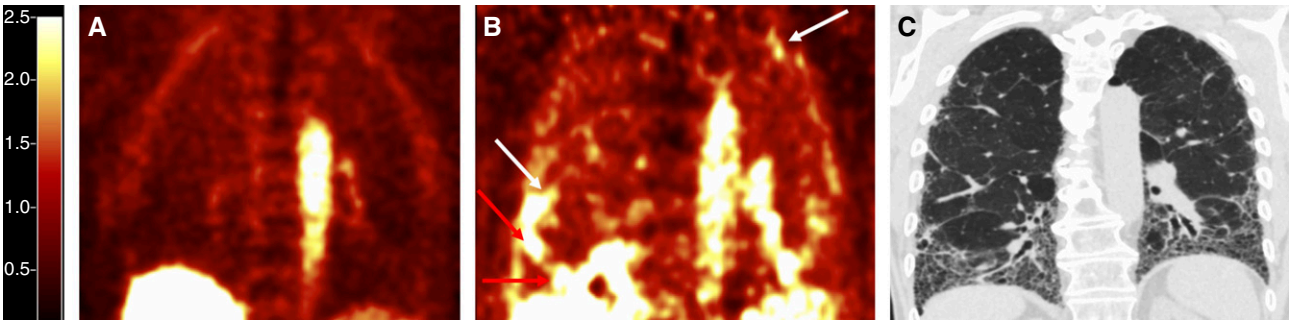

Figure 2. Collagen-targeted molecular imaging using ^{68}Ga-CBP8 positron emission tomography (PET). (*A*) Coronal PET image of a healthy volunteer, demonstrating low collagen tracer signal in the lungs. (*B*) PET image of a subject with idiopathic pulmonary fibrosis rendered on the same scale as in *A*, demonstrating areas of high collagen tracer signal predominantly in subpleural and basilar regions in the lungs. (*C*) High-resolution computed tomography (CT) of the same subject with idiopathic pulmonary fibrosis obtained within 8 weeks of PET–magnetic resonance imaging. Compared with the PET imaging (*B*), increased collagen tracer signal is not confined to areas of fibrosis visualized on CT. White arrows highlight regions of high tracer signal within areas of lung without apparent fibrosis on CT. Red arrows highlight regions of high tracer signal within areas of established fibrosis on CT.

skin and bone even though both tissues had an abundance of type I collagen. Furthermore, within explanted IPF lung tissue, there was less ^{68}Ga-CBP8 uptake in end-stage honeycomb cysts than in less advanced fibrotic areas. As collagen becomes more organized into fibers, it provides fewer binding sites for ^{68}Ga-CBP8 than freshly synthesized and disorganized collagen.

We detected increased collagen tracer signal within areas of known fibrosis and regions where fibrosis was not apparent by CT. These preliminary results suggest that areas of high collagen tracer signal represent active or recent collagen synthesis and that ^{68}Ga-CBP8 PET may detect active collagen deposition that is not yet visible, thus serving as a viable disease activity measure. Although we did not validate our results histologically or confirm ^{68}Ga-CBP8's specificity for collagen in this study, we have strong data from two mouse models of pulmonary fibrosis and explanted IPF lungs demonstrating that ^{68}Ga-CBP8 accurately and specifically detects the presence of collagen (1). Additional studies are needed to determine whether ^{68}Ga-CBP8 can predict IPF disease progression and detect early response to antifibrotic therapies, and how ^{68}Ga-CBP8 compares to other PET tracers, such as ^{18}F-fluorodeoxyglucose, when applied to pulmonary fibrosis. Given that type I collagen is a hallmark of fibrosis across organ systems, ^{68}Ga-CBP8 may have wide-ranging clinical applicability for fibrosis imaging. ■

Author disclosures are available with the text of this letter at www.atsjournals.org.

Acknowledgment: The authors thank Dr. Leo Ginns, Stephanie Koo, Sunakshi Paul, and the entire PET and MRI team of the Athinoula A. Martinos Center for Biomedical Imaging for their assistance.

Sydney B. Montesi, M.D.*
David Izquierdo-Garcia, Ph.D.
Massachusetts General Hospital
Boston, Massachusetts
and
Harvard Medical School
Boston, Massachusetts

Pauline Désogère, Ph.D.
Eric Abston, M.D., Ph.D.
Lloyd L. Liang, B.A., M.S.
Massachusetts General Hospital
Boston, Massachusetts

Subba Digumarthy, M.D.
Massachusetts General Hospital
Boston, Massachusetts
and
Harvard Medical School
Boston, Massachusetts

Ravi Seethamraju, Ph.D.
Siemens Healthineers
Boston, Massachusetts

Michael Lanuti, M.D.
Peter Caravan, Ph.D.
Ciprian Catana, Ph.D., M.D.
Massachusetts General Hospital
Boston, Massachusetts
and
Harvard Medical School
Boston, Massachusetts

ORCID IDs: 0000-0002-3179-6537 (P.C.); 0000-0002-3249-5971 (C.C.).

*Corresponding author (e-mail: sbmontesi@partners.org).

References

1. Désogère P, Tapias LF, Hariri LP, Rotile NJ, Rietz TA, Probst CK, *et al*. Type I collagen-targeted PET probe for pulmonary fibrosis detection and staging in preclinical models. *Sci Transl Med* 2017; 9:eaaf4696.
2. Montesi SB, Izquierdo-Garcia D, Abston E, Désogère P, Digumarthy SR, Seethamraju R, *et al*. Collagen-targeted PET imaging in idiopathic pulmonary fibrosis: first-in-human studies [abstract]. *Am J Respir Crit Care Med* 2019;199:A7349.
3. Montesi SB, Rao R, Liang LL, Goulart HE, Sharma A, Digumarthy SR, *et al*. Gadofosveset-enhanced lung magnetic resonance imaging to detect ongoing vascular leak in pulmonary fibrosis. *Eur Respir J* 2018; 51:1800171.
4. Montesi SB, Désogère P, Fuchs BC, Caravan P. Molecular imaging of fibrosis: recent advances and future directions. *J Clin Invest* 2019;129: 24–33.

5. Désogère P, Montesi SB, Caravan P. Molecular probes for imaging fibrosis and fibrogenesis. *Chemistry* 2019;25:1128–1141.
6. John AE, Luckett JC, Tatler AL, Awais RO, Desai A, Habgood A, *et al*. Preclinical SPECT/CT imaging of αvβ6 integrins for molecular stratification of idiopathic pulmonary fibrosis. *J Nucl Med* 2013;54: 2146–2152.
7. Ambrosini V, Zompatori M, De Luca F, Antonia D, Allegri V, Nanni C, *et al*. 68Ga-DOTANOC PET/CT allows somatostatin receptor imaging in idiopathic pulmonary fibrosis: preliminary results. *J Nucl Med* 2010; 51:1950–1955.
8. Win T, Thomas BA, Lambrou T, Hutton BF, Screaton NJ, Porter JC, *et al*. Areas of normal pulmonary parenchyma on HRCT exhibit increased FDG PET signal in IPF patients. *Eur J Nucl Med Mol Imaging* 2014;41: 337–342.
9. Withana NP, Ma X, McGuire HM, Verdoes M, van der Linden WA, Ofori LO, *et al*. Non-invasive imaging of idiopathic pulmonary fibrosis using cathepsin protease probes. *Sci Rep* 2016;6:19755.
10. Win T, Screaton NJ, Porter JC, Ganeshan B, Maher TM, Fraioli F, *et al*. Pulmonary ^{18}F-FDG uptake helps refine current risk stratification in idiopathic pulmonary fibrosis (IPF). *Eur J Nucl Med Mol Imaging* 2018;45:806–815.
11. Wynn TA. Cellular and molecular mechanisms of fibrosis. *J Pathol* 2008;214:199–210.

Digital Lung Auscultation: Will Early Diagnosis of Fibrotic Interstitial Lung Disease Become a Reality?

To the Editor:

Interstitial lung diseases (ILDs) are a heterogeneous group of lung disorders that are often associated with substantial morbidity and early mortality. Pulmonary fibrosis is characteristic of most ILDs, and preliminary data suggest that early diagnosis and prompt intervention can improve clinical outcomes (1).

Idiopathic pulmonary fibrosis (IPF), one of the most common and best-studied forms of ILD, has a median estimated survival of 2–5 years from diagnosis (2). Delayed referral to a tertiary care center may be associated with higher mortality, irrespective of disease severity (3).

Early detection is essential to establish an accurate diagnosis and ensure timely intervention with appropriate treatment, as there are antifibrotics that have been approved for IPF (pirfenidone and nintedanib) and are effective in slowing disease progression (4) but do not reverse fibrosis. In addition, the decline in lung function for patients with IPF and preserved lung volume seems to be similar to that observed in those with more impaired lung volume (∼200 ml/yr), and both groups appear to benefit equally from antifibrotic treatment (5).

Furthermore, patients with advanced IPF are more likely to discontinue treatment (6), adding to the rationale for earlier intervention. Here we discuss the potential role of digital lung auscultation as an aid to support the early identification of patients with suspected fibrotic ILD.

Early Diagnosis of IPF Is Challenging

Most patients experience significant challenges in their pursuit of a correct diagnosis of IPF (7). The nonspecific symptoms of IPF, including cough and insidiously progressive dyspnea, usually lead to repeated physician visits and multiple diagnostic tests, with misdiagnoses being commonplace (7).

Specific diagnostic procedures, such as chest high-resolution computed tomography (HRCT) to detect the patterns of usual interstitial pneumonia, lung biopsy, and multidisciplinary discussions, are recommended for an accurate diagnosis of IPF. Consideration of demographic and clinical data also improves diagnostic confidence (8).

Identification of interstitial lung abnormalities (ILAs), defined as the presence of specific patterns on chest computed tomography, may offer a strategy for early detection of IPF (9). The feasibility of this approach is dependent on an improved understanding of ILA subgroups and the nature of disease progression (9).

Rationale for the Use of Digital Lung Auscultation

Earlier access to a tertiary care center might be facilitated by improved methods of lung sound detection, including the recognition of so-called "Velcro-like" crackles, a hallmark feature that is present early in the disease course of IPF and in many fibrotic ILDs (10).

A subjective assessment of Velcro-like crackles bilaterally on chest auscultation predicts the presence of fibrotic ILD and usual interstitial pneumonia patterns on HRCT (10, 11), and is associated with varying degrees of different ILAs (10). Hence, Velcro-like crackles may provide a rationale for investigating lung sounds to accurately identify patients with ILD, and could even be used as a screening aid. It has been suggested that the presence or absence of fine Velcro-like crackles at lung auscultation should be considered in the management of subjects with (sub)clinical ILD (12).

Methods for quantitative analysis of lung sounds have been shown to distinguish the Velcro-like crackles found in IPF from the lung sounds present in other pulmonary conditions that cause similar symptoms (13); research in this area is ongoing.

There is a clear need for further, clinically oriented, prospective studies to clarify the limitations and potential of the existing data. Previous studies have been affected by extensive variability in the methods used and features investigated; the complexity of the recording systems used (e.g., multichannel analyzers and air-coupled sensors); and a lack of robust diagnostic research designs for small, preselected study populations, usually with inappropriate reference to diagnostic standards.

Steps Needed to Bring Digital Lung Auscultation into Clinical Practice

Research projects are under way to build more evidence in this field. In an ongoing, multicenter clinical trial (clinicaltrials.gov identifier: NCT03503188), digital lung sounds and basic patient characteristics are being prospectively collected from patients with IPF and symptom-matched control subjects. A well-established teaching device for lung sounds (14) will be used as a reference.

Author Contributions: L.R., V.C., G.W., M.K., and G.S. contributed to the background literature search, providing appropriate references for inclusion. L.R., M.K., M.C., and G.S. suggested inclusion of the figure and provided input into how digital auscultation might fit into the algorithm for management of patients with idiopathic pulmonary fibrosis. All authors contributed to development of the manuscript in terms of critical review and amendment of initial drafted content, and approved the final submitted version.

Originally Published in Press as DOI: 10.1164/rccm.201902-0306LE on May 31, 2019